

Energetics and efficiencies of collision-induced dissociation achieved during the mass acquisition scan in a quadrupole ion trap

Glen P. Jackson*, Jennifer J. Hyland and Ünige A. Laskay

Center for Intelligent Chemical Instrumentation, Department of Chemistry and Biochemistry, Ohio University, Athens, OH 45701-2979, USA

Received 13 September 2005; Revised 4 October 2005; Accepted 4 October 2005

Using *n*-butylbenzene as a test molecule, evidence is provided that fast, efficient or highly energetic collision-induced dissociation (CID) can be achieved during the mass acquisition ramp of a commercially available quadrupole ion trap (QIT) mass spectrometer. The method of excitation is very similar to axial modulation for mass range extension except that lower amplitude waveforms are used to excite the precursor ions within the trap instead of ejecting them from the trap. ITSIM simulations verify that fast kinetic excitation followed by kinetic-to-internal energy transfer occurs on the rapid time-scale required for the recapture and mass analysis of product ions during the mass acquisition ramp. CID efficiencies larger than 50% can be obtained using this new approach and ratios of Th 91/92 of *n*-butylbenzene fragment ions as large as 9 are possible, albeit at significantly reduced efficiencies. These very large ratios indicate an internal energy above 7 eV for the precursor ions indicating that fragmentation of larger ions could also be possible using this new approach. The main benefits of the new method are that no extra time is required for fragmentation or cooling and that on-resonance conditions are guaranteed because the ions' secular frequencies are swept through the fixed frequency of excitation. Also presented are the effects of experimental variables such as excitation frequency, excitation amplitude and scan rate on the CID efficiencies and energetics. Copyright © 2005 John Wiley & Sons, Ltd.

Quadrupole ion traps (QITs) are widely recognized for their flexibility and sensitivity in accomplishing tandem mass spectrometry (MS/MS), which is an invaluable tool for the quantitative, qualitative and mechanistic interrogation of gas-phase ions.^{1,2} The ability to perform MS/MS is important because it is a central technology for proteomics^{3,4} and applications such as drug/metabolite monitoring and forensic sciences.^{1,5,6} Most applications of MS/MS rely on the ability to obtain reproducible and reliable fragmentation spectra from selected precursor ions in order to match database entries or to make other dependable conclusions based on the fragmentation spectra. However, faster and more complex separation technologies are being developed that demand MS/MS spectra to be obtained more quickly and on smaller sample sizes than is favorable for reliable on-resonance excitation to be performed. These new demands require fresh approaches for achieving MS/MS while, if possible, not adding to the complexity or cost of the instrumentation.

*Correspondence to: G. P. Jackson, Center for Intelligent Chemical Instrumentation, Department of Chemistry and Biochemistry, Ohio University, Athens, OH 45701-2979, USA.
E-mail: jacksong@ohio.edu
Contract/grant sponsor: Office of the Vice President for Research and the College of Arts and Sciences at Ohio University.

On-resonance excitation using supplemental alternating current (ac)-waveforms applied to the end-cap electrodes has been the most widely used approach for achieving collisional activation of selected precursor ions. This method of fragmentation is available on almost all modern commercially available instruments and has been extremely well characterized. For example, the performance of on-resonance excitation has been found to be dependent on a number of experimental variables including excitation amplitude,^{7–14} excitation duration,^{8–14} the trapping parameter of the precursor ion (q_z) or product ion,^{11,12,15,16} the excitation frequency,^{10,12,17} the buffer gas,^{18,19} cooling periods prior to fragmentation,^{20–22} and the number of ions in the trap (space charge).²³ Although on-resonance excitation in QITs has proven extremely valuable from a qualitative point of view, the variety of factors that influence the ability to ensure on-resonance conditions has largely precluded its use as a quantitative on-resonance excitation in QITs. On-resonance conditions are especially complicated to attain in the presence of higher-order fields in the QIT because ions tend to shift secular frequencies in the process of being excited.² For these reasons, attempts at quantitative collision-induced dissociation (CID) measurements using on-resonance excitation such as threshold determinations^{7,17} or bond-strength determinations have found limited success.^{7,17,24} Because of the limitations of on-resonance excitation – such as

optimization time, excitation time and fragmentation efficiency – alternative fragmentation methods are continually being sought.

Of the alternative electrodynamic approaches to on-resonance excitation, boundary-activated dissociation (BAD)^{15,18,25,26} and direct current (dc) excitation^{27–32} have been amongst the most widely studied. BAD has the advantage that product ions spanning a wide range of m/z values can be efficiently recaptured following CID. However, BAD suffers from the limited amount of internal energy that can be imparted to precursor ions. Pulsed dc excitation can impart large amounts of internal energy into precursor ions in a very short time, but the timing of the applied dc pulses (5–20 μ s in length) with respect to the phase of the ion motion of the precursor ion is critical.³⁰ It is therefore non-trivial to apply dc-pulse excitation to isolated precursor ions on the time-frame of a chromatographic separation. In another approach to CID, Murrell *et al.* recently introduced 'fast CID'²⁹ which uses high-amplitude on-resonance excitation for short periods of tens to hundreds of microseconds. Conventional on-resonance fragmentation times are on the order of tens of milliseconds. 'Fast CID' has the advantage that precursor ions can be excited at an optimum low mass cut-off (LMCO) value for energy deposition whereas the product ions can be collected at a different LMCO value to optimize their collection efficiency. However, this approach still requires on-resonance conditions to be optimized prior to excitation, so the problems associated with on-resonance conditions do not seem to have been alleviated.

Instrument manufacturers use a variety of approaches to overcome the problems associated with establishing on-resonance conditions. Bruker Daltonics uses a broad band of excitation frequencies³⁵ applied to the end-cap electrodes to ensure that the molecular ions pick up resonant energy from one or more of the waveforms, even if the secular frequencies of the molecular ions shift during the excitation period. Thermo Finnigan uses an approach of modulated secular-frequency excitation³³ wherein the trapping amplitude is continually increased and decreased to cycle the secular frequency of the molecular ions back and forth through the fixed single-frequency excitation waveform on the end-cap electrodes. Other approaches include red shift off-resonance large amplitude excitation,³⁴ and random-noise excitation,³⁶ neither of which appears to have found widespread application. Each of the above approaches requires an independent scan period devoted to collisional activation which can lengthen the time required to obtain a product ion spectrum. When ion signals are stable and exist for a significant length of time, the above approaches are perfectly adequate at providing CID spectra of selected precursor ions. However, when precursor ion signals are transient – such as when eluting from a gas chromatography (GC) or high-performance liquid chromatography (HPLC) column – significant benefits can be gained by shortening the time required to obtain a product ion spectrum. In these cases, eliminating or shortening the extra scan periods enables more product ion spectra to be obtained during the lifetime of the transient precursor ion signal.

Previous studies have shown that in the process of axial modulation during mass acquisition – in order to eject ions at

a position in the stability diagram away from the boundary at $\beta = 1$ ($q_z = 0.908$) – fragile ions are often found to fragment as they absorb power from the applied waveform.^{37–44} Uncontrolled fragmentation of this kind during mass acquisition is usually considered to be problematic because it causes peak fronting or peak shifts. However, some groups have used the peak fronting to interrogate the fragility of selected ions.^{41,44} To our knowledge, until recently,⁴⁵ there were no reports on the *intentional* fragmentation of precursor ions during mass acquisition. However, it is found that when smaller amplitudes of axial modulation are used to excite ions during the mass analysis scan, product ions can indeed be recaptured and scanned out at a meaningful m/z value – as long as the frequency of excitation is far enough away from the stability boundary to recapture the product ions.⁴⁵ In this report, we have refined the technique of CID during mass acquisition and examine the effects of certain parameters on the fragmentation behavior.

In order to obtain better insight into the energetics of CID during mass acquisition the *n*-butylbenzene molecular ion at 134 Th was used as a precursor 'thermometer' ion. The fragmentation behavior of *n*-butylbenzene has been extensively studied and the fragmentation pathways and thermodynamics are well known.^{10,11,15,16,21,22,27,31,46–53} By observing the ratios of product ions at 91 and 92 Th the new fragmentation method is shown to provide comparable information to on-resonance excitation with several noteworthy benefits: (1) on-resonance conditions are guaranteed without any prior tuning or calibration and (2) significant time savings are possible in the new approach because no extra scan events are required other than ionization, isolation and mass acquisition periods. This new approach to achieving fragmentation of selected precursor ions is expected to be universally applicable to inorganic, organic and biological ions, the latter of which are the focus of continuing investigations.

EXPERIMENTAL

A Thermo Finnigan Polaris Q quadrupole ion trap mass spectrometer (San Francisco, CA, USA) with a Trace GC oven was used without any hardware modifications to collect all the experimental data. The test compound, *n*-butylbenzene (99% purity, Sigma-Aldrich, St. Louis, MI, USA), was infused through the GC transfer line at a controlled rate using a needle valve and a short length of 30 μ m i.d. silica capillary which sampled the headspace of \sim 2 mL of the undiluted *n*-butylbenzene in a septum-capped glass vial. The vial containing the *n*-butylbenzene was located in the Trace GC oven and held at a constant temperature of 50°C. Ions were formed in the unmodified EI source and injected and collected in the trap for a duration of 0.5 ms unless otherwise noted. Software programs were written in Visual Basic[®] 6.0 (Redmond, WA, USA) using the XCalibur development kit (XDK) command language provided by Thermo Electron Corp. The flexibility available in the command language and electronic boards greatly assisted in writing software that is capable of performing 'looped' or sequence-linked experiments that run consecutively, without user intervention. This capability was invaluable for collecting data from consecutive

experiments that differ only in the value or magnitude of one variable. The Polaris Q is set up to allow two waveforms to be applied to the end-cap electrodes at any given time. One of these waveforms is a single-frequency waveform and this is used to generate the 470 kHz signal to achieve axial modulation close to the stability boundary. The other waveform was used to achieve excitation of the ions at an arbitrarily selected point in the stability diagram during mass acquisition. The excitation waveforms were generated using a hand-written arbitrary waveform generating program and stored as a digital array in the XDK source code. The waveform array contains 4000 data points and is clocked out at 2 ms (50 ns per data point). The waveform is applied continuously, back-to-back, at a desired amplitude for the duration of the mass analysis scan.

The data shown in Figs. 4–6 were collected in individual sequence-looped experiments. For example, in Fig. 4, the first loop of the program generates ions and injects them into the trap, isolates them using a LMCO value and frequency notch waveform provided by the existing software, and mass analyzes them at a scan rate of 0.18 ms/Th with an axial modulation frequency and amplitude provided by the software (approximately 470 kHz). In this first loop of the experiment, an additional axial modulation frequency of 171 kHz and 0.0 V is applied to the end caps during mass acquisition. The raw data is stored in the XCalibur software and selected ion intensities are exported to an Excel spreadsheet. The program then automatically moves to the second loop of the experiment in which all the same sequence of events is repeated except that the excitation amplitude at 171 kHz is stepped to 0.1 V. The program continues until the selected excitation amplitude limit is reached (3.0 V in this case). In all the programs written almost any variable can be predefined at the start of the sequence-looped experiment. These fixed variables include the precursor ion mass-to-charge value, isolation width and isolation time, cool time prior to mass acquisition, the LMCO start and finish values for mass acquisition, the scan rate during mass acquisition, excitation amplitude during mass acquisition, excitation frequency during mass acquisition, start and finish excitation amplitudes during mass acquisition, and step size between these amplitudes. The data shown in Fig. 6 used a similar program, but this time the excitation amplitude was held constant for each loop of the program and the excitation frequency was incrementally increased in each loop. Another similar program was written to loop through different scan rates at a fixed excitation amplitude and frequency, but the changes in mass calibration and signal intensity at the different scan rates require more intricate data manipulation. No data using this latter program are shown in this report.

ITSIM 5.0 simulation software available from the Cooks research group at Purdue University was used to simulate the experiments.⁵⁴ The modeling was based on initial conditions of 20 precursor ions of *n*-butylbenzene ions at 300 K with a hard-sphere cross section set at 50 Å. The bath gas was helium at a pressure of 1 mTorr and temperature of 300 K. Integration parameters were set as follows; method: 4th order Runge-Kutta; integration step: 10 ns; collision probability: hard-sphere model with random-angle-scattering enabled; internal energy calculated from average of collisions. The LMCO

was ramped from 40 to 150 Th at a fixed frequency of 1.03 MHz. Dipolar excitation of 171 kHz was applied at the desired voltage for the duration of the mass acquisition step (20 ms). The resulting enveloped data was exported to Excel for plotting.

RESULTS AND DISCUSSION

Figure 1 compares the scan functions for performing CID of selected precursor ions in a conventional on-resonance excitation approach and for the new approach. In essence, the new method of fragmenting precursor ions is identical to performing axial modulation for mass-range extension,⁵⁵ with the only exception that the amplitude of the axial modulation waveform on the end-cap electrodes is reduced to minimize the ejection of ions at the selected point of excitation. In addition to the excitation waveform applied to the end caps during mass acquisition, an axial ejection waveform close to $q_z = 0.9$ is still applied – as it is in the conventional mode for mass acquisition. Thus, during mass acquisition, a total of two fixed frequency waveforms are applied in a dipolar fashion to the end-cap electrodes: one at a low frequency (100–200 kHz) and small amplitude to effect fragmentation and one at a higher frequency (~470 kHz) and large amplitude to effect ejection of the ions. The times shown are approximate and relate to mass acquisition from 40–150 Th at a regular scan rate of 0.18 ms/Th (5.5 Th/ms). Although the new approach could offer significant time savings when

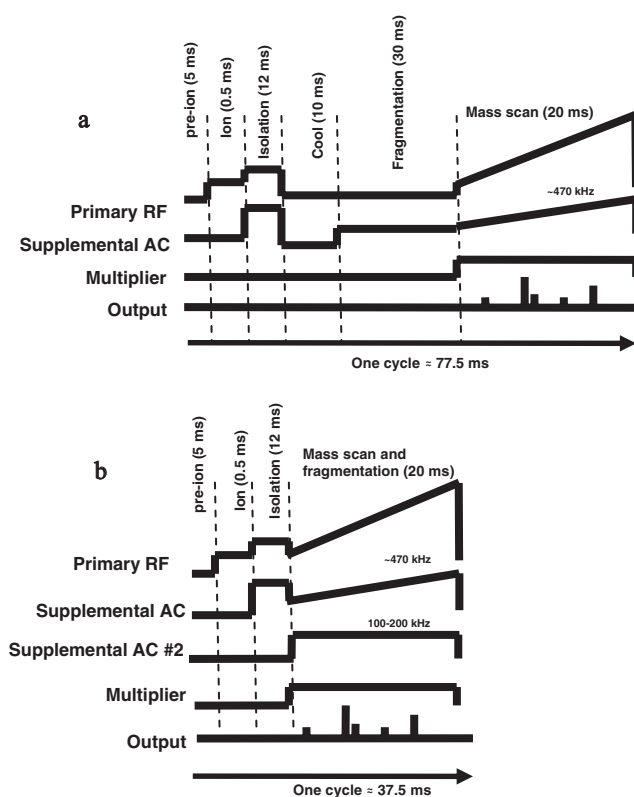


Figure 1. Typical scan functions used for (a) conventional on-resonance excitation of an isolated precursor ion and (b) the proposed method of exciting an isolated precursor ion during mass acquisition.

the ionization times are very short, the percentage time savings will be much smaller when the ionization time increases.

In a conventional on-resonance excitation experiment the LMCO of the ring electrode must be carefully selected to ensure that the secular frequency of the ions is resonant with the excitation frequency applied to the end caps. If the frequency of the ions is not resonant with the frequency on the end-cap electrodes, fragmentation efficiencies may deteriorate and product distribution intensities may vary. Inconsistent or faulty resonance tuning can therefore lead to inconsistent results between experiments or between instruments. In the new approach, an excitation waveform of, say, 171 kHz ($q_z = 0.45$) and 1.0 V in amplitude is applied to the end-cap electrodes continuously during mass acquisition. As the isolated precursor ions are scanned from a LMCO of, say, 40 to 150 Th, the n-butylbenzene ions at 134 Th will be resonant with the applied frequency when the LMCO is approximately 67 Th (LMCO = $134 \text{ Th} \times 0.45 / 0.908 = 134 / 2$).² Therefore, when the LMCO reaches ~ 67 Th, the n-butylbenzene ions will be kinetically excited by the on-resonance waveform until the LMCO reaches a value slightly above 67 Th, when the ion frequency becomes non-resonant with the applied waveform. The kinetic energy picked up by the ions as they are swept through on-resonance conditions is converted into internal energy via inelastic collisions with the helium bath gas. Fragment ions having a mass-to-charge ratio greater than the value of the LMCO value at their time of formation will be recaptured in the trap, whereas product ions having mass-to-charge values less than the LMCO value at their time of formation will be unstable and ejected. As was demonstrated earlier,⁴⁵ if the precursor ions gain too much kinetic energy as they pass through the excitation waveform, they too can become unstable and will be ejected. Ejected precursor ions therefore show up at a LMCO value that corresponds to the time when they are on-resonance with the excitation waveform. In the above example, the n-butylbenzene ions at 134 Th will be ejected at a LMCO of 67.

Figure 2 shows mass spectra obtained when isolated n-butylbenzene ions are mass-analyzed with an additional excitation waveform of 171 kHz applied to the end-cap electrodes. Figure 2(a) shows that when an excitation amplitude of 0.0 V is applied, no fragmentation of the precursor ions is observed, as expected. Figure 2(b) shows that when the excitation amplitude is increased to 2.0 V, a significant amount of fragmentation is observed at the expected product ion masses of 91, 92, 105 and 119 Th. This spectrum demonstrates that product ions are successfully recaptured and mass-analyzed in the time taken for the product ions to reach the edge of the stability diagram. At an excitation amplitude of 171 kHz, the precursor ions come into resonance when the LMCO is at 67 Th. At a scan rate of 0.18 ms/Th, we estimate that the product ions at 91 Th will be trapped for a maximum time of 4.3 ms. According to the spectrum shown in Fig. 2(b), this is sufficient time for the ions to obtain a stable trajectory with normal peak position, width and symmetry. As indicated in Fig. 1, the spectrum shown in Fig. 2(b) was obtained in a scan time of 37.5 ms. A typical MS/MS experiment using on-resonance excitation to achieve a similar result would take approximately 77.5 ms, depending on the excitation time, to achieve similar results. The

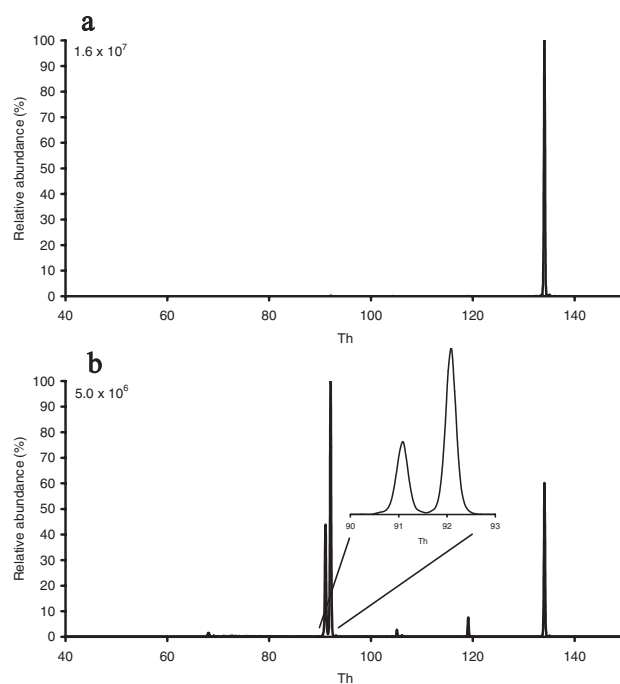


Figure 2. Mass spectra showing the deliberate fragmentation of precursor ions and mass analysis of product ions when n-butylbenzene ions are excited during mass acquisition using dipolar excitation of (a) 0.0 V and (b) 2.0 V at 171 kHz ($q_z = 0.45$).

new approach could therefore offer significant time savings compared to conventional on-resonance excitation, while providing similar fragmentation product distribution ratios. In certain cases, conventional on-resonance excitation periods as short as 1.5 ms have been demonstrated to be capable of inducing effective fragmentation of the same n-butylbenzene precursor ion.⁴⁷ Compared to these short excitation times, the new approach proposed here does not offer significant time savings. However, the new approach does offer the advantage that no resonant tuning is required: the ions are guaranteed to become non-resonant with the applied frequency at some point during the mass scan. In addition, the time between product ion formation and detection is much shorter in the new approach than the conventional manner, which could help prevent unwanted secondary reactions of the product ions.¹¹

Figure 3 shows the results of two simulation experiments that mimic the experimental conditions examined in Fig. 2. Figures 3(a) and 3(b) show the z kinetic energy (end-cap dimension) and internal energy, respectively, calculated for 20 n-butylbenzene ions with an excitation waveform of 0.0 V and 171 kHz applied to the end caps during the mass acquisition scan. The simulation shows that, as expected, the ions do not pick up significant kinetic or internal energy until they reach the edge of the stability diagram when the LMCO approaches 134 Th at ~ 18 ms. Figures 3(c) and 3(d) show the z kinetic energy and internal energy under identical conditions, but with an excitation waveform of 2.0 V and 171 kHz applied to the end caps during mass acquisition. In this case, the ions pick up significant kinetic

energy when the ions come into resonance with the applied frequency at approximately 5 ms (LMCO = 67). This kinetic energy is converted to internal energy via collisions with the helium bath gas, as demonstrated by the increase in internal energy after 5 ms in Fig. 3(d). In the simulation experiments, fragmentation of the precursor ions was disabled. In reality, when the internal energy of the precursor ions exceeds the threshold of fragmentation energy of ~ 1 eV,⁵⁰ the ions would ordinarily fragment. In agreement with the experimental observations, the simulation results show that within a short time (2–4 ms) after kinetic excitation, the precursor ions gain enough internal energy to effect fragmentation before the product ions reach the stability boundary.

Figure 4 shows the effect of excitation amplitude on the relative ion abundances when precursor ions of *n*-butylbenzene are excited at a frequency of 171 kHz ($q_z = 0.45$) during mass acquisition.

The general trend in fragmentation behavior with excitation amplitude shown in Fig. 4 is very similar to that observed using conventional on-resonance excitation with the exception that the threshold amplitude for fragmentation is shifted to higher amplitudes in the new approach. The competition between resonance excitation and resonance ejection is well known⁹ in conventional on-resonance excitation in QITs and the theory is equally relevant to the fragmentation approach used here. At small excitation amplitudes, no fragmentation is observed. At approximately 0.8 V amplitude, fragmentation becomes apparent and the product ion at 92 Th is observed. As the excitation amplitude increases, the precursor ion signal decreases and the product ion signals increase to a maximum intensity at around 2 V. Ejection of the precursor ions becomes apparent at ~ 2.2 V and reaches a maximum around 3 V. The total ion current (TIC) is found to decrease as the excitation amplitude increases, even though a significant proportion of the ejected ions are detected when the LMCO passes a value of 67 Th. The reduction in TIC is

presumably due to ejection in a dimension different to the direction of the detector, although this is difficult to determine experimentally. We are currently using the ITSIM simulation software to assist with this determination, but we have not determined if the ions are ejected axially, towards the entrance end cap, or radially, towards the ring electrode.

The toluene-like product ion at 92 Th is formed via a rearrangement reaction and has a threshold energy of 0.99 eV.⁵⁰ The bond-cleavage product ion at 91 Th has a higher threshold energy of 1.61 eV, but is kinetically favored when excess internal energy is available. For this reason, when *n*-butylbenzene precursor ions are heated slowly by multiple low-energy collisions in the QIT,⁵⁶ the lowest energy channel resulting in 92 Th product ions is most favorable. When higher energy methods of activation are used – such as single, high-energy collisions, charge-transfer reactions or photodissociation reactions – the 91 Th product ion is most favorable. Therefore, the ratio of Th 91/92 is found to provide a convenient way of determining the internal energy of the precursor ions at the time of fragmentation. Large Th 91/92 ratios indicate larger internal energies and smaller Th 91/92 ratios indicate smaller internal energies.

Figure 5 shows the ratio of Th 91/92 as a function of excitation amplitude using a frequency of 171 kHz applied to the end caps during mass acquisition. In agreement with previous experiments,^{10,11,47,48} it is found that the ratio of Th 91/92 increases with increasing excitation amplitude, indicating that the ions obtain larger internal energies prior to fragmentation at higher excitation amplitudes. Also plotted on this figure is the CID efficiency, defined as the percentage conversion of precursor ions into product ions. The CID efficiency is normalized to the TIC present when the excitation amplitude is at 0.0 V, so the efficiencies do include the ejected ions that are not detected by the conversion dynode. Figure 5 shows that, under these specific conditions, the CID efficiency reaches a maximum of 50% at around 2.0 V.

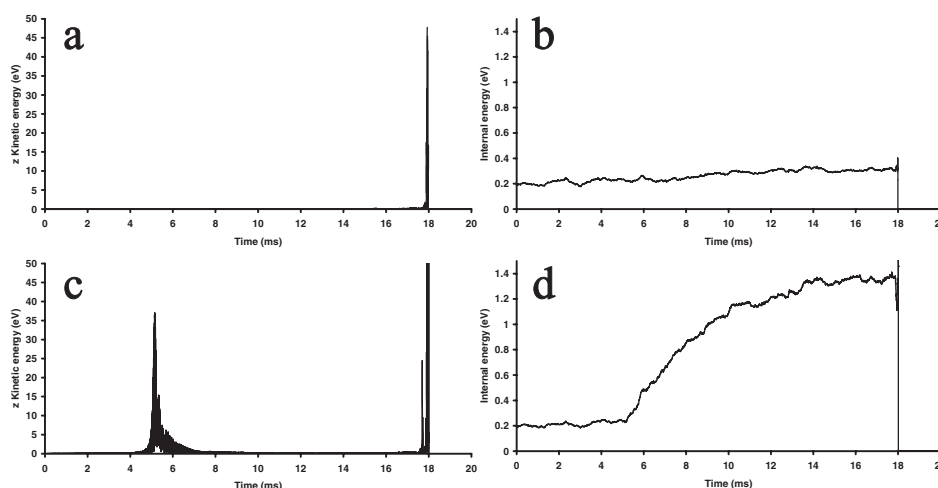


Figure 3. ITSIM simulation results of the experiments performed to obtain the data shown in Fig. 2. (a, b) The *z* kinetic energy and internal energy, respectively, as a function of time when *n*-butylbenzene ions are excited with an amplitude of 0.0 V during mass acquisition. (c, d) Results obtained when an excitation waveform of 2.0 V at 171 kHz is applied to the end caps during mass acquisition.

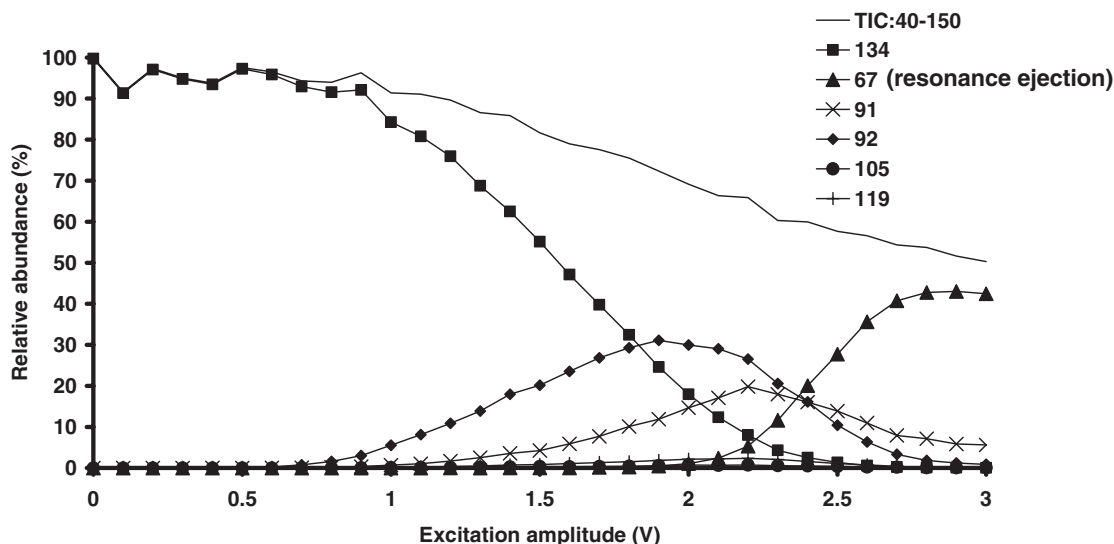


Figure 4. Plot of the relative abundance of ions versus the excitation amplitude when n-butylbenzene ions are excited at a frequency of 171 kHz during mass acquisition.

As the excitation amplitude increases above 2.0 V ejection becomes more prominent and the CID efficiencies decrease. At the largest excitation amplitude of 3.5 V the CID efficiency reaches a minimum of $\sim 5\%$, which remains almost constant even at higher amplitudes. This 'efficiency' at higher amplitudes was originally thought to be due to the fragile nature of the n-butylbenzene ion, but close inspection shows that the product ions are due to the high-energy fragmentation channel resulting in 91 Th product ions. Excitation amplitudes up to 5.0 V have been studied at this frequency, but complete resonance ejection does not seem to be possible under the conditions employed. The lack of complete ejection could be due to space-charge effects or some other factor perturbing ion trajectories.⁴⁰

At the maximum CID efficiency of 50%, the Th 91/92 ratio is approximately 1. To achieve this same ratio using conventional on-resonance excitation, Liere *et al.* used an excitation amplitude of $\sim 0.7 V_{pp}$ at $q_z = 0.4$ for 10 ms. The CID efficiency under their conditions was approximately 30%, albeit under conditions that may not have been optimized. The new approach therefore seems to offer similar energy conversion with better efficiency and shorter analysis time than the conventional approach. The largest ratio Th 91/92 observed by Liere *et al.* was ~ 2.5 at an excitation amplitude of 1 V. At this amplitude the CID efficiency remained almost unchanged at $\sim 25\%$. Using the new method of CID during mass acquisition, the CID efficiency at a Th 91/92 ratio = 2.5 is slightly worse at $\sim 20\%$. Therefore, using the new approach, it

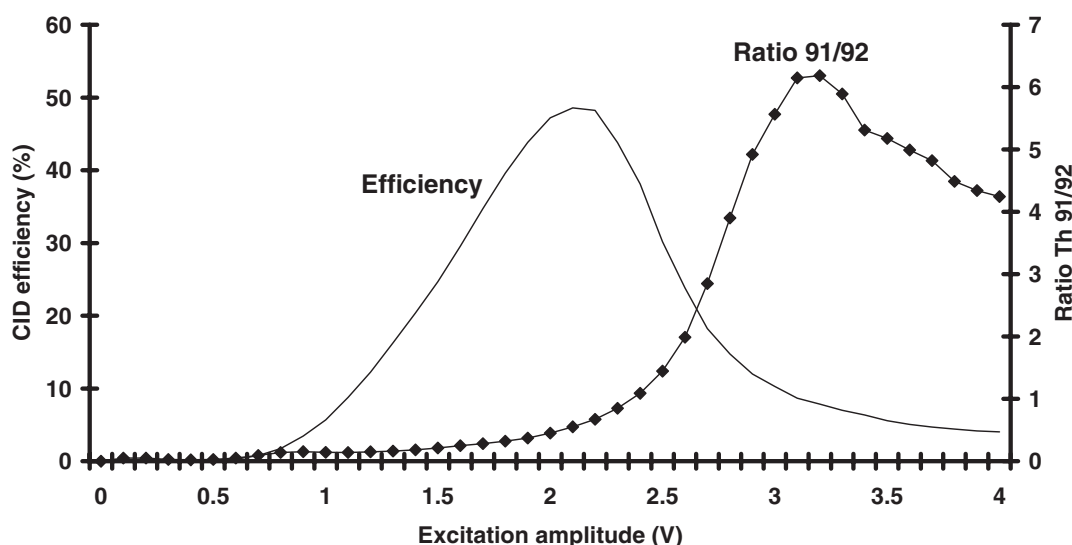


Figure 5. Plot of experimentally determined CID efficiency and Th 91/92 ratio as a function of excitation amplitude when n-butylbenzene ions are fragmented at a frequency of 171 kHz during mass acquisition.

is possible to obtain Th 91/92 ratios as high as 7, corresponding to an internal energy of approximately 6.5 eV.⁵⁰ At these very high internal energy conditions, CID efficiencies are considerably reduced to around 10%. This observed Th 91/92 ratio and concomitant CID efficiency exceeds the largest ratios and associated efficiencies obtained using normal on-resonance excitation in a QIT.⁴⁸ However, this Th 91/92 ratio of 7 does not quite reach the extreme Th 91/92 ratio of 20 obtained recently in a QIT using large pulsed dc amplitudes.^{27,28}

In order to better understand the instrumentation factors affecting the new method of fragmentation, we studied the effects of applied frequency (read stability parameter) and scan rate on the energetics and CID efficiencies. Figure 6 shows the CID efficiencies and Th 91/92 ratios obtained as a function of excitation frequency. The excitation amplitude was fixed at 3.0 V and the scan rate was 0.18 ms/Th. At this large excitation amplitude CID efficiencies are relatively poor because of the significant degree of ejection of the precursor ions. The precursor ion signals (not shown) are below 10% of the relative abundance at all frequencies, indicating that fragmentation or ejection is significant. The LMCO value at which ejection occurs varies as a function of excitation frequency, and the ejection signal is found to be strongest at the lowest frequencies studied. This is expected because the ions are trapped in a smaller Dehmelt pseudopotential well depth at lower q_z values.² At a frequency of 225 kHz ($q_z = 0.57$) the LMCO value at which the precursor ions come into resonance with the applied frequency is at ~ 87 Th. The product ion signals at this excitation amplitude become severely degraded and display significant peak tailing on the low mass side. This is indicative of the fact that the product ions have only just been formed and are occupying unstable trajectories before being resonantly ejected from the trap near the stability boundary at $q_z = 0.9$. At frequencies above 250 kHz, the LMCO value at which the precursor ion comes into resonance with the applied frequency occurs

above 92 Th, so any product ions formed at 91 or 92 Th show up as an ejection signal at the corresponding LMCO value. Without prior knowledge of the fragmentation products of a given precursor ion, one must be careful to assign the peak at the ejection LMCO to pure ejection of the precursor ion; it is possible that part of the ejection signal will be due to fragmentation products that have a mass-to-charge value smaller than the LMCO value at the time of formation.

Figure 7 shows the effect of scan rate on the CID efficiencies and Th 91/92 ratios as a function of excitation amplitude when an excitation frequency of 171 kHz is applied to the end-cap electrodes during mass acquisition. As before, the CID efficiencies are determined by calculating the percentage of product ion signals at given excitation amplitude relative to the total ion signal at 0.0 V excitation at the given scan rate. The CID efficiencies were normalized to the 0.0 V point at each scan rate because the absolute signal intensities are considerably larger at faster scan rates;⁵⁷ e.g. with the ion time set at a constant 0.5 ms, the TIC at a scan rate of 0.1 ms/Th is approximately 12 times larger than at a scan rate of 0.9 ms/Th. In general, the slower scan rates require smaller excitation amplitudes to achieve efficient fragmentation of the precursor ions. This is because, at slower scan rates, the precursor ions are moving more slowly through the frequency domain and will therefore spend a longer time being resonant with the fixed frequency of excitation. At faster scan rates, the precursor ions move more quickly through the frequency domain and the ions pass very quickly through resonance conditions, so the ions will not have as much time to become kinetically excited by the applied waveform. Therefore, larger excitation amplitudes are required at faster scan rates to impart a similar degree of energy to the ions as the slower scan rates.

At all the scan rates studied, CID efficiencies are 0% with an excitation amplitude of 0.0 V. The CID efficiency increases with increasing excitation amplitude up to a maximum amplitude that is dependent on the scan rate. At the slowest

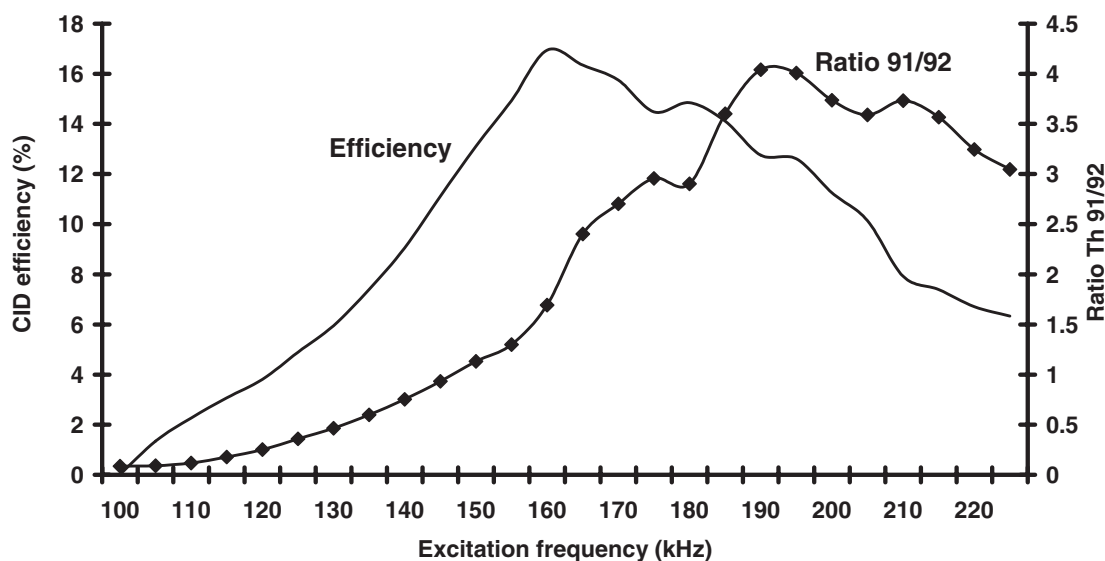


Figure 6. Plot of the CID efficiency and Th 91/92 ratio as a function of excitation frequency at a scan rate of 0.18 ms/Th and excitation amplitude of 3.0 V.

scan rate examined of 0.9 ms/Th ($5 \times$ slower than the default), the CID efficiency maximizes at a relatively small excitation amplitude of ~ 1 V. At the fastest scan rate of 0.1 ms/Th, the CID efficiency maximizes at much larger excitation amplitudes of ~ 3.0 V. The maximum CID efficiency at each scan rate differs slightly, and reaches an overall optimum value of 50% around 0.36 ms/Th. From the raw spectra (not shown), one can see that the slower scan rates lead to slightly more ejection when the precursor ions come into resonance with the excitation waveform, whereas the faster scan rates lead to slightly less ejection and a lesser degree of fragmentation. For all the scan rates observed, excitation amplitudes less than the amplitude at the maximum CID efficiency display less ejection signal and more precursor ion signal. For excitation amplitudes larger than the amplitude at the maximum CID efficiency, the spectra show decreasing precursor ion signals and increasing ejection ion signals. An interesting note is that at large excitation amplitudes the CID efficiencies tend to reach a minimum value at each scan rate and do not decrease with a further increase in excitation amplitude. This indicates that a certain number of product ions are formed and trapped even at the largest amplitudes studied.

A close examination of the CID efficiency at frequencies from 110–210 kHz and 4.0 V excitation (not shown) indicated that CID efficiencies reached a minimum of $\sim 1\%$ at lower frequencies (hence lower q_z during excitation) and a maximum of $\sim 8\%$ at an excitation frequency around 171 kHz. CID efficiencies decreased to another minimum of $\sim 5\%$ at an excitation frequency of 210 kHz. The CID efficiencies reveal that the default scan rate of 0.18 ms/Th is close to the scan rate at which the maximum possible CID

efficiency can be achieved using single-frequency excitation during mass acquisition. Different precursor ions could have different optimum scan rates and this is expected to be related to the lowest mass fragments that are produced in the fragmentation process.

The Th 91/92 ratios plotted in Fig. 7(b) were extracted from the same spectra from which Fig. 7(a) was constructed. If one looks at the excitation amplitude required to reach a Th 91/92 ratio of 2, one can clearly see that the slower scan rates achieve this ratio at lower excitation amplitudes. There does not appear to be a general trend in the maximum Th 91/92 ratio at each scan rate, or a general trend in the Th 91/92 ratio once the maximum ratio is obtained. For example, the Th 91/92 ratio at the slowest scan rate of 0.9 ms/Th reaches a minimum after the first maximum and reaches a second maximum at ~ 3.3 V. In contrast, the Th 91/92 ratio at a scan rate of 0.36 ms/Th remains quite constant after reaching the maximum ratio of ~ 7 . Different again is the behavior at scan rates of 0.14 and 0.18 ms/Th, which show well-defined maxims in the Th 91/92 ratios. The largest Th 91/92 ratio of >9 was observed at a scan rate of 0.14 ms/Th and an excitation amplitude of 3.5 V. This Th 91/92 ratio exceeds the limits of the calibration curve obtained using photodissociation methods, and is thought to be one of the largest ratios yet obtained using axial modulation in a QIT. This ratio corresponds to an internal energy above 7 eV at the time of fragmentation. This is not expected to be an average internal energy of all the precursor ions because many of them are ejected before they fragment. However, the observed ratio gives a good indication of the internal energy of precursor ions whose fragmentation products can be recaptured and mass-analyzed in the time-frame of mass acquisition. The fast time-frame for excitation at the faster scan rates is thought to closely resemble fast dc pulse or fast ac pulse excitation,^{27,29,58} as demonstrated by the simulation in Fig. 3.

The CID efficiency at the Th 91/92 ratio of 9 is quite poor at $\sim 5\%$. However, at a scan rate of 0.36 ms/Th, Th 91/92 ratios as large as 7 are consistently obtained with CID efficiencies in excess of 10%. Fortuitously, the default scan rate of 0.18 ms/amu appears to provide an optimal balance between CID efficiency, the ability to impart large internal energy to the ions and the ability to obtain fragmentation spectra as fast as possible. Faster scan rates could impart even more energy to ions but at a loss of collection efficiency. Alternatively, slower scan rates could provide more complete, but lower energy fragmentation. An interesting trade-off worth noting is that the enhanced signal-to-noise ratios of ion signals at the faster scan rates could make up for the lower CID efficiencies at the faster scan rates. A detailed study of the minimum quantity of precursor from which product ion spectra can be obtained would be an obvious next step for investigation. A final consideration when using different scan rates is the mass resolution obtained in the resulting spectra. It is well known that by slowing the scan rate of the rf voltage ramp, enhanced peak resolution in excess of 30 000 m/ δm (~ 0.003 full width at half maximum (FWHM) at 91 Th) can be made possible.^{55,59} At the default scan rate of 0.18 ms/Th, mass resolution of product ions at 91 Th formed during mass acquisition is approximately 0.21 (FWHM), as shown in Fig. 2(b). At the slowest scan rates (0.9 ms/Th) mass

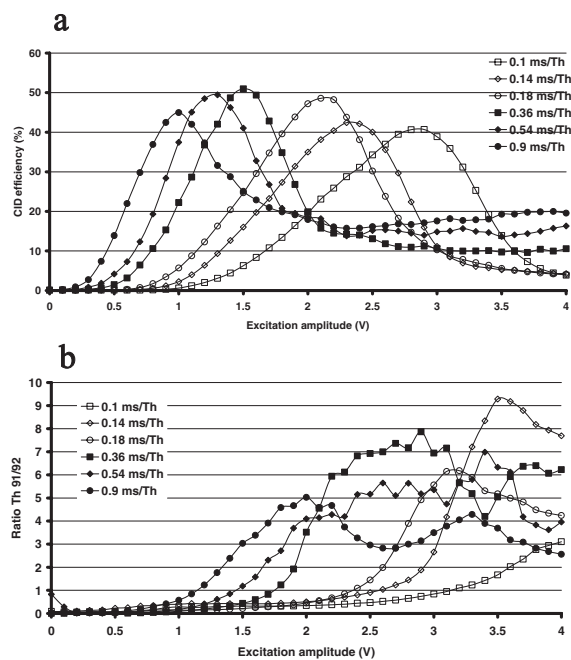


Figure 7. Plot of CID efficiency and Th 91/92 ratio as a function of excitation amplitude at several different scan rates. The CID efficiencies at each scan rate are calculated relative to the precursor ion signal at 0.0 V at each scan rate.

resolution of the peak at 91Th improves to a little under 0.12Th (FWHM, data not shown). Therefore, even for product ions formed during the mass acquisition ramp, enhanced peak resolution can be obtained by using slower scan rates.

These preliminary studies show that this new method of activating precursor ions and mass analyzing the fragmentation products could hold significant promise in selected applications. The new technique is expected to be optimal when the difference in mass-to-charge between the precursor ions and product ions is smallest, just as these conditions are more favorable for conventional on-resonance excitation. An obvious extension of this work is to consider using multiple frequencies during the mass acquisition ramp to effect higher energy fragmentation or more efficient CID of the precursor ions. Indeed, initial results (not shown) indicate that multiple frequencies are more beneficial with respect to CID efficiency and energy deposition. The results of multiple-frequency excitation during mass acquisition are intended for subsequent publications.

Acknowledgements

Olivier Collin is gratefully recognized for his assistance with the VB programming. GPJ is grateful to Lei Li, Douglas E. Goeringer and Douglas C. Duckworth for their contributions during the early stages of this work. We thank the Cooks group at Purdue University for the use of the ITSIM 5.0 software. Finally, the Office of the Vice President for Research and the College of Arts and Sciences at Ohio University are gratefully acknowledged for start-up funds.

REFERENCES

1. Busch KL, Glish GL, McLuckey SA. *Mass Spectrometry/Mass Spectrometry: Techniques and Applications of Tandem Mass Spectrometry*. VCH Publishers: New York, 1988.
2. March RE, Todd FJ. *Quadrupole Storage Mass Spectrometry*. John Wiley: New York, 1989.
3. Yates JR. *J. Mass Spectrom.* 1998; **33**: 1.
4. Graves PR, Haystead AJ. *Microbiol. Mol. Biol. Rev.* 2002; **66**: 39.
5. Marquet P. *Ther. Drug Monit.* 2002; **24**: 255.
6. Griffiths WJ. *Mass Spectrom. Rev.* 2003; **22**: 81.
7. Colorado A, Brodbelt J. *J. Am. Chem. Soc. Mass Spectrom.* 1996; **7**: 1116.
8. Goeringer DE, Asano KG, McLuckey SA. *Int. J. Mass Spectrom.* 1999; **182/183**: 275.
9. Charles MJ, McLuckey SA, Glish GL. *J. Am. Soc. Mass Spectrom.* 1994; **5**: 1031.
10. Liere P, March RE, Blasco T, Tabet J-C. *Int. J. Mass Spectrom. Ion Processes* 1996; **153**: 101.
11. Liere P, Steiner V, Jennings KR, March RE, Tabet J-C. *Int. J. Mass Spectrom. Ion Processes* 1997; **167/168**: 735.
12. Gronowska J, Paradisi C, Traldi P, Vettori U. *Rapid Commun. Mass Spectrom.* 1990; **4**: 306.
13. Constantin E, Schnell A, Guidugli F, Traldi P. *Org. Mass Spectrom.* 1992; **27**: 174.
14. Paradisi C, Traldi P, Vettori U. *Rapid Commun. Mass Spectrom.* 1993; **7**: 690.
15. Paradisi C, Todd JFJ, Vettori U. *Org. Mass Spectrom.* 1992; **27**: 1210.
16. Steiner V, Beaugrand C, Liere P, Tabet J-C. *J. Mass Spectrom.* 1999; **34**: 511.
17. Hart KJ, McLuckey SA. *J. Am. Soc. Mass Spectrom.* 1994; **5**: 250.
18. Paradisi C, Todd JFJ, Traldi P, Vettori U. *Org. Mass Spectrom.* 1992; **27**: 251.
19. Danell RM, Danell AS, Glish GL, Vachet RW. *J. Am. Soc. Mass Spectrom.* 2003; **14**: 1099.
20. Duckworth DC, Goeringer DE, McLuckey SA. *J. Am. Soc. Mass Spectrom.* 2000; **11**: 1072.
21. Liere P, Bouchonnet S, March RE, Tabet J-C. *Rapid Commun. Mass Spectrom.* 1995; **9**: 1594.
22. Liere P, Blasco T, March RE, Tabet J-C. *Rapid Commun. Mass Spectrom.* 1994; **8**: 953.
23. Alheit R, Kleinedam S, Vedel F, Vedel M, Werth G. *Int. J. Mass Spectrom. Ion Processes* 1996; **154**: 155.
24. Jackson GP, King FL, Goeringer DE, Duckworth DC. *Int. J. Mass Spectrom.* 2002; **216**: 85.
25. Paradisi C, Todd JFJ, Traldi P, Vettori U. *Rapid Commun. Mass Spectrom.* 1992; **6**: 641.
26. Asam MR, Glish GL. *J. Am. Soc. Mass Spectrom.* 2002; **13**: 650.
27. Lammert SA, Cooks RG. *Rapid Commun. Mass Spectrom.* 1992; **6**: 528.
28. Julian RK, Nappi M, Weil C, Cooks RG. *J. Am. Soc. Mass Spectrom.* 1995; **6**: 57.
29. Murrell J, Despeyroux D, Lammert SA, Stephenson JL, Goeringer DE. *J. Am. Soc. Mass Spectrom.* 2003; **14**: 785.
30. Plass WR. *Int. J. Mass Spectrom.* 2000; **202**: 175.
31. Wang MD, Schachterle S, Wells G. *J. Am. Soc. Mass Spectrom.* 1996; **7**: 668.
32. Splendore M, Lausevic M, Lausevic Z, March RE. *Rapid Commun. Mass Spectrom.* 1997; **11**: 228.
33. Mila L, Splendore M, March RE. *J. Mass Spectrom.* 1996; **31**: 1244.
34. Qin J, Chait BT. *Anal. Chem.* 1996; **68**: 2108.
35. Julian RK, Cooks RG. *Anal. Chem.* 1993; **65**: 1827.
36. McLuckey SA, Goeringer DE, Glish GL. *Anal. Chem.* 1992; **64**: 1455.
37. Dobson G, Murrell J, Despeyroux D, Wind F, Tabet J-C. *J. Mass Spectrom.* 2005; **40**: 714.
38. Dobson G, Murrell J, Despeyroux D, Wind F, Tabet J-C. *J. Mass Spectrom.* 2004; **39**: 1295.
39. Dobson G, Murrell J, Despeyroux D, Wind F, Tabet J-C. *Rapid Commun. Mass Spectrom.* 2003; **17**: 1657.
40. Favre A, Gonnet F, Tabet J-C. *Rapid Commun. Mass Spectrom.* 2001; **15**: 446.
41. McClellan JE, Murphy JP, Mulholland JJ, Yost RA. *Anal. Chem.* 2002; **74**: 402.
42. Murphy JP, Yost RA. *Rapid Commun. Mass Spectrom.* 2000; **14**: 270.
43. Splendore M, Marquette E, Oppenheimer J, Huston C, Wells G. *Int. J. Mass Spectrom.* 1999; **191**: 129.
44. Vachet RW, Hartman JAR, Callahan JH. *J. Mass Spectrom.* 1998; **33**: 1209.
45. Jackson GP, King FL, Duckworth DC. *J. Anal. At. Spectrosc.* 2003; **18**: 1026.
46. Goeringer DE, McLuckey SA. *Rapid Commun. Mass Spectrom.* 1996; **100**: 328.
47. Basic C, Yost RA. *Int. J. Mass Spectrom.* 2000; **194**: 121.
48. Louris JN, Cooks RG, Syka JEP, Kelly PE, G. C. Stafford J, Todd JFJ. *Anal. Chem.* 1987; **59**: 1677.
49. Oh ST, Choe JC, Kim MS. *J. Phys. Chem.* 1996; **100**: 13367.
50. Baer T, Dutuit O, Mestdagh H, Rolando C. *J. Phys. Chem.* 1988; **92**: 5674.
51. Chen JH, Hays JD, Dunbar RC. *J. Phys. Chem.* 1984; **88**: 4759.
52. Dawson PH. *Int. J. Mass Spectrom. Ion Processes* 1985; **63**: 339.
53. McLuckey SA, Ouwerkerk CED, Boerboom AJH, Kistemaker PG. *Int. J. Mass Spectrom. Ion Processes* 1984; **59**: 85.
54. Bui HA, Cooks RG. *J. Mass Spectrom.* 1998; **33**: 297.
55. Kaiser RE, Cooks RG, Stafford GC, Syka JEP, Hemberger PH. *Int. J. Mass Spectrom. Ion Processes* 1991; **106**: 79.
56. McLuckey SA, Goeringer DE. *J. Mass Spectrom.* 1997; **32**: 461.
57. Yang CG, Bier ME. *Anal. Chem.* 2005; **77**: 1663.
58. Cunningham C, Remes PM, Burinsky DJ, Glish GL. *Proc 53rd ASMS Conf. Mass Spectrometry and Allied Topics*, San Antonio, TX, 2005.
59. Schwartz JC, Syka JEP, Jardine I. *J. Am. Soc. Mass Spectrom.* 1991; **2**: 198.